Paper Review Report

A Review of Towards Collaborative Drilling with a Cobot Using Admittance Controller

Transparency Optimization of the Galen Surgical System with a Frequency Domain Admittance Controller Design

Brevin Banks

Table of Contents:

1. Project Statement

This project aims to optimize the transparency of the Galen robotic surgical system using a frequency-based admittance controller while keeping the robot stable during human and environment interactions. The situation highlighted by this project is what is called a pHRI system which is meant by a physical human robot interaction system. The proposed outcome of this project is a controller that works on both the simulated robot hardware in MATLAB SIMULINK and AMBF and the real Galen robot hardware in the mock OR. This will be accomplished by control systems design in MATLAB and by analyzing the stability of different control schemes for different values of m and b (the desired admittance mass and damping) that will result in an increased transparency observed by the human user. Incidentally, a stability map and impedance cost map,

addressed here later, will be generated that allow for future improvement of this control design for the Galen robot to be performed and even expanded to other robots. Ultimately, the improvement in transparency will allow the operator or surgeon to use the robot with lower human effort required than currently experienced with the Galen robot, and the system should be more stable over all regions of the workspace.

2. Paper Selection

1. The paper selected, *A Review of Towards Collaborative Drilling with a Cobot Using Admittance Controller* (Aydin et al 2020), contains a control scheme that features an admittance controller of the type identical to the desired model for our Galen control design. A cobot is a robot that is designed to interact with humans either through hand over hand interaction or close proximity. This paper was chosen because it outlines the fundamental features of the design of an admittance controller, uses stability and cost impedance maps to predict the desired performance of the robot, and utilizes system dynamics type identification of the robot in a convenient and universal way. The methods and results show how the transparency and stability of any pHRI system can be measured and improved with expected experimental results.

3. Summary of Goal, Key Results, and Significance

Transparency and stability go hand in hand whilst actively opposing one another. When interacting with a cobot, is best when the user can move as freely as possible regarding the impedance felt by the robot inertia and joints. The impedance or resistance is tiring and not optimal for improving the pHRI experience. Consequently, admittance controllers implement features to remove the impedance at the risk of lowering the stability of the robot dynamics. Stability observes the regions where the robot is likely to track inputs well or where the robot will take inputs and drive somewhere unbounded, unstable, and most likely dangerous. The reason admittance may drive controllers unstable is because they impose a desired virtual mass and damping over the robot dynamics, effectively removing the robot dynamics, and replacing them with new values and rely on feedback and filtering to keep the output stable. With too small a desired admittance masses and damping the controller becomes closer and closer to dividing by zero and sending the output velocity, position, or force to unstable and over saturating values. Special caution must be taken in the control design to select appropriate values of m and b to keep the system stable yet transparent and this paper explains the process to do so.

They also include a system identification analysis of the LBR robot to obtain a simplified linear form of the dynamics to use with easy integration of an admittance controller. Although this has relevance to our need to identify the system behavior on the Galen as well, the main goal of both our project and this paper are to apply admittance controllers

to any linear system, therefore the system identification portion of this review will be highly summarized. For explicit details see the paper.

The authors used an admittance controller on a single cartesian direction of an LBR iiwa 7 R800 robot (KUKA Inc.), an industrial robot arm, to allow a human to interact with a drill attached to the robot end effector. The goal was to observe the human effort required to drill a hole in a piece of wood using different permissible values for the admittance controller desired mass m and desired damping b.

The key results of the work are the obtained stability and transparency maps that allow any controller designer to select m and b values that will keep the robot stable and transparent for any desired task. The result of the experiment is a stable working admittance controller in one cartesian dimension. They also show how different values of m and b affect the human effort, and make suggestions on how to choose better m and b values.

4. Necessary background

There is no critical prior work done by the authors that is needed to understand the workflow of this paper, but a fundamental background in basic linear control theory and understanding of some key terms are required. In the case that fundamental topics of linear control theory are well understood, it is recommended to move on to section 5.

A basic overview for linear control theory is an expansive topic that can be studied from resources like *Feedback Control of Dynamic Systems,* Franklin Ed[8][4], but an extremely simplified example will be given by the simplified block diagram of the feedback controller below.

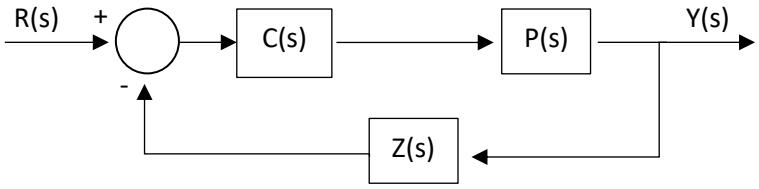

Figure 1 A simple feedback block diagram of a control system with input R(s) and output Y(s)

In the above diagram, there are 5 different variables. R is an input, this could be a desired force, velocity, position, etc. Y is the desired output. If you're controlling a robot, then it could be the output velocity of the different joints. The other variables within the diagram are designed to monitor and implement the input R to achieve the desired output Y. The block Z represents an impedance. It could be some form of resistance due to the environment, a human touching the robot, or the robot itself. When the line from Y goes through Z and back to R by the circle comparator block, we call this feedback. In other

words, the desired output, Y, is affected by an external impedance, Z, and fed by to the input R, to see if they agree. The large circle with a + and – near it is a comparator. It takes the difference between the input R and the output Y*Z and evaluates the error between them. It should be noted that we can multiply Y and Z as such to obtain the effects of impedance on the output. This works in the case that R, is an input force and Y is an output velocity. Also note that this controller is designed in the frequency domain. Hence each term has (s) following it and we work in the Laplace domain. This means this controller works in continuous time, or 'ideal conditions' if the robot sampling rate was infinite. This makes quick analysis of the control system easier than solving for real time or discrete solutions although it may not reflect performance on real discrete hardware. See more on control theory for details on this.
Continuing the explanation of the diagram elements, C is a controller. It features some user tuned variables that help pull the error between R and YZ closer to 0. Finally, we have P, the plant. It is essentially the dynamics of whatever needs to be controlled. In our case this is the robot. If we assume the robot is a linear system, it can be imagined as a mass spring damper or set of mass spring dampers that take in an input force and output a position or velocity.

Finally, a transfer function is a ratio between any input or output types in a control scheme. It essentially states that for a given input you will get a predicted output. For the diagram above we can find the transfer function multiply through the input and output to each block. We start with Y feedback through Z to get YZ, then take the difference between YZ and R to get (R-YZ). Then we can multiply this by C and P to get Y.
i.e. (R-YZ)CP = Y. By solving for $\frac{Y(s)}{R(s)}$ the closed loop transfer function for the diagram above is:

$$\frac{Y(s)}{R(s)} = \frac{C(s)P(s)}{1+Z(s)C(s)P(s)} \qquad \text{(Eq.1}$$

This is useful because we can use the denominator of the transfer function to determine if the resultant control scheme will be stable. The denominator will result in a linear polynomial of variable 's' that can be solved. The solutions to the polynomial are called 'poles' of the transfer function, and by investigating their values, stability can be determined. If any real part of a pole is a positive number, the system will go unstable. If all the real parts of the poles are negative the system will be stable.

This concludes the brief summary of basic feedback control theory and will provide enough background to clarify the approach used in the paper.

5. Technical Approach

a. Controller

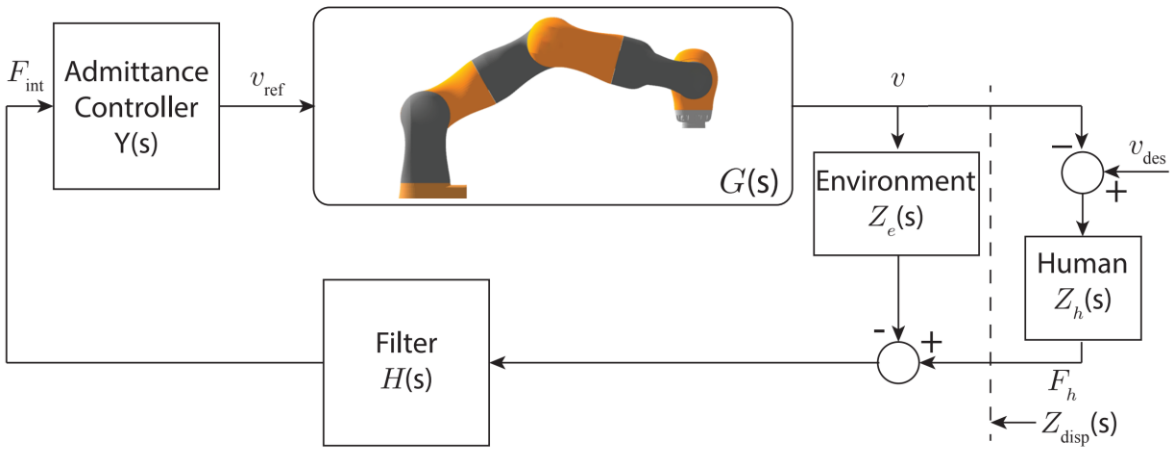

Figure 2 Admittance Control Scheme used in the paper [1]

Figure 2 features the control scheme utilized to include admittance, and the resultant transfer function is:

$$T(s) = \frac{V(s)}{F_{\text{ref}}(s)} = \frac{G(s)Y(s)}{1 + G(s)Y(s)H(s)Z_{\text{eq}}(s)} \quad \text{(Eq.2}$$

Each parameter in the diagram above will be explained below.

b. Admittance

This closed loop control system has Y(s) that functions as a sort of plant of its own. The structure of Y(s) is:

$$Y(s) = \frac{1}{ms+b} \quad \text{(Eq.3}$$

Where m and b are the desired admittance mass and damping the user should be feeling. This is the tunable parameter newly introduced to the control scheme that should help the controller feel more transparent.

c. Filtering

H(s) is a low pass 2nd order Butterworth filter with a cutoff frequency of 5Hz. It was included mostly to remove noise and spikes in impedance changes.

d. System Identification

G(s) features the identified dynamics of the robot. To obtain G(s) the robot LBR robot was analyzed between 0.01Hz and 20Hz (the estimated range of possible human hand frequencies) where an estimated linear time invariant system (LTI) was produced. This is done by moving the robot to sinusoidal reference positions and recording the output. Identification can be done by taking the input sinusoids and outputs and comparing the two in system identifier software that will produce a linear transfer function between inputs and outputs. Because this was done on a robot with an onboard position controller, the dynamics identified here include both the plant and controller. This means that G(s) = C(s)P(s)

e. Impedance

Because cobots interact with humans and the environment, the estimated impedance values for the human and environment are included in Zh(s) and Ze(s) respectively. The authors chose to estimate these values as mass spring dampers based on prior work in the literature that found bounded values on the maximum human impedance. The work of Buerger et al. (2007) found the maximum values of human impedance to be mh = 5kg, bh = 41 Ns/m, and kh = 401 N/m where impedance takes the form $Zh(s) = m_h s + b_h + \frac{k_h}{s}$ for a velocity controller [2]. Similarly, they identified the top environment impedance as only a stiffness where ke=16499 N/m where impedance takes the form $Ze(s) = \frac{k_e}{s}$
For the design of the controller it is important to differentiate Zh(s) and Ze(s), but in stability and transparency analysis it is okay to think of the two parallel elements as one equivalent impedance $Zeq(s) = m_h s + b_h + \frac{k_h}{s} + \frac{k_e}{s}$

f. Stability

The range of values for the impedance are important because the impedance of the human and environment affect the overall stability of the controller. If the user co-contracts their arm muscle they can increase the stiffness or damping in the impedance which would cause the system to lean unstable. Humans also come in different sizes, and their reflexes respond differently to different types of feedback from the robot. Similarly, if the user

suddenly let's go of the robot the system is completely devoid of impedance. All of these can wildly change the response of the system dynamics rather quickly. Given the range of scenarios the authors decided to evaluate the stability of the system in 2 situations over a range of 4 different impedance criterion. The first was to evaluate the stability with the human and the environment both interacting simultaneously (a situation where the human would be holding the robot while the robot is drilling or touching something in the room). This would be done with 4 different impedance cases. 1 mh = 5kg, bh = 41 Ns/m, 2 mh = 0kg, bh = 41 Ns/m, 3 mh = 5kg, bh = 0 Ns/m, and 4 mh = 0kg, and bh = 0 Ns/m. The stiffness for the human is all left the same at kh = 401 N/m. The second situation was similar to the first, only the environment stiffness is removed, and only the human interactions are considered. Again, the same 4 impedance cases were used to assess the stability of the system.

Stability was determined by looking at the closed loop transfer function poles for both situations and all impedance cases while adjusting the values of m and b. The result was these stability maps.

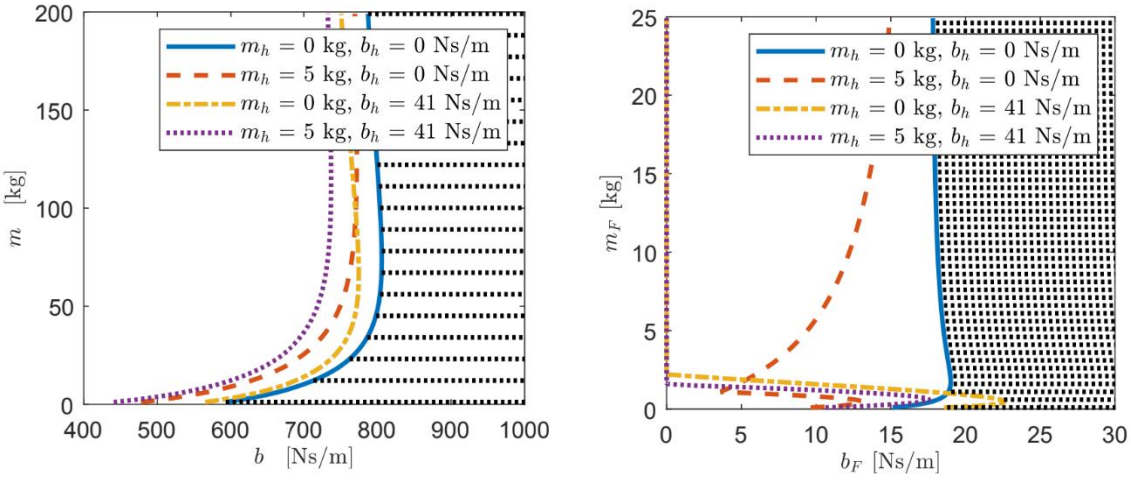

Figure 3 stability maps for different desired admittance values of m and b. Left if with environment stiffness ke = 16499 N/m Right is with environment stiffness ke = 0 N/m. The shaded areas represent regions of stability. [1]

They found that the case with high environment impedance and only human stiffness to be the most extreme bounding case where the controller would be most unstable. As seen in Figure 3 on the left, in blue is the case where the environment impedance is present, but only the human stiffness is interacting. The shaded area is where the controller is deemed stable for all forms of interaction. In Figure 3 on the right is the situation without environment impedance, and it can be observed that m and b are permissibly lower than for cases with environment impedance as anticipated. Therefore, regarding controller design, the authors suggest that choosing the most transparent values of m and b within the stable range of Figure 3 on the left will result in the most optimal stable controller.

g. Transparency

To choose optimal values of m and b the authors proposed using a measurement of parasitic impedance to represent transparency. By evaluating the open loop transfer function through cutting out the portion of the controller to the right of Zdisp(s) in figure 2 and subtracting the environment impedance, the result is the parasitic impedance function.

$$|\Delta Z(j\omega)| = 1/|G(j\omega)Y(j\omega)H(j\omega)| \quad \text{(Eq.4}$$

The magnitude of parasitic impedance is a quantitative measurement of how much impedance the human is feeling by the cobot. The authors take a weighted sum of this magnitude over the range of possible human hand frequencies (0.01Hz to 30Hz) to produce a cost map of the parasitic impedance for different values of m and b.

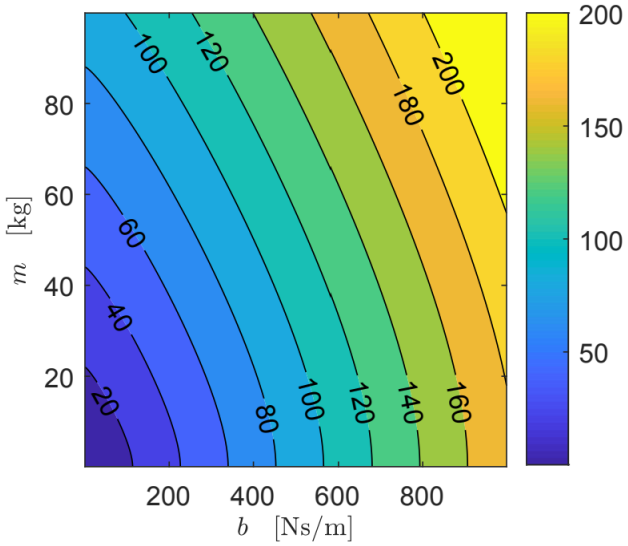

Figure 4 Cost map for the parasitic impedance of the control system seen by the human for different desired admittance values m and b. Blue means that the cost is lower, the impedance is lower, and the transparency is higher [1].

Figure 4 shows this cost map for the parasitic impedance. Areas that are in blue represent areas of low impedance and high transparency. Areas that are more yellow, represent areas of high impedance and low transparency.
The evaluation of parasitic impedance becomes every more valuable when the stability map from figure 3 on the left is overlayed on its results.

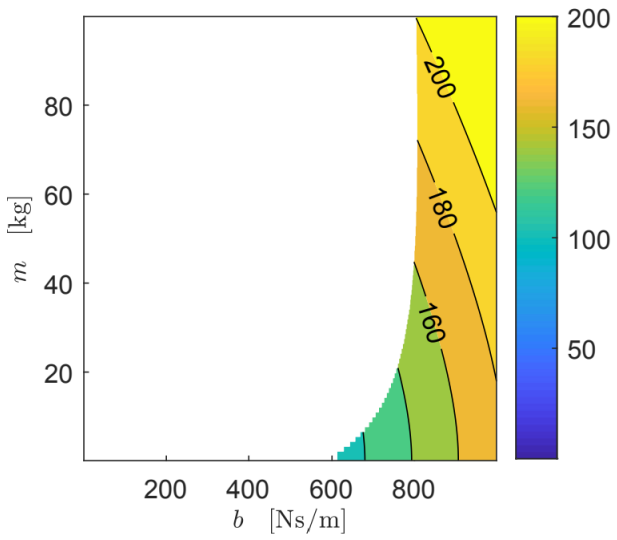

Figure 5 Transparency cost map with stability overlayed. This combined plot shows where the control system in figure 2 is stable and what the permissible m and b values are in coordination with their relative transparency. Yellow is less transparent; blue is more transparent. Only values in the colored region are allowed [1].

This map shows where a control system designer working with an LBR robot can select values of m and b for the admittance controller where stability is guaranteed. Using this map, the authors selected several m and b value combinations in the acceptable region and observed their effects on the effort of the human while drilling in a piece of wood.

6. Experimental Evaluation and Results

The authors tested the following 3 sets of values for m and b in the stable transparent range from figure 5.

	m [kg]	b [Ns/m]
I	20	1500
II	20	900
III	50	900

Figure 6 The selected test values for desired admittance m and b [1]

Case 1 features high damping with a low mass. Case 2 features lower damping and mass. Case 3 features high mass and low damping. Using these values, the authors setup 3 different controllers and placed a wooden work piece in the path of robot. The robot end effector was fixed with a drill and some force sensors to observe the human effort. The depth of the drill in the work piece was also observed with some external sensors and feedback about the relative depth of the drill tip to the desired depth was relayed back to the user in an AR headset interface.

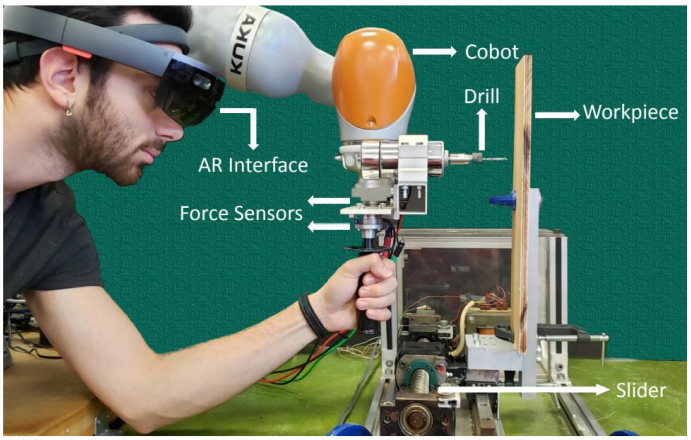

Figure 7 Procedure setup with robot in one direction. The user pushes the robot into the wooden workpiece. The AR interface relates back to them how close the drill tip is to the desired drill depth [1].

Each case was repeated 4 times leaving 12 cases in total to examine. The results for the measured forces and velocities were averaged for each case and plotted with their standard deviations as seen in figure 8.

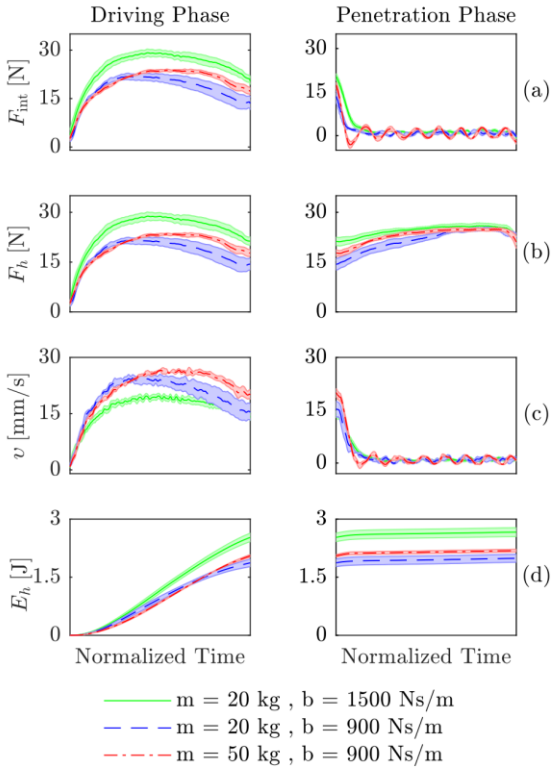

Figure 8 The output for cases 1 through 3. Fint is the interaction force between the human the robot, Fh is the force of the human, v is velocity out, Eh is the effort of the huma. Averages plotted with standard deviations in the lighter regions. [1].

The most pertinent figures in the results are the output velocity and the human effort. The output velocity shows how the performance of the controller effects the robot, and the

human effort reflects the difficulty for the human to achieve the desired position. It can be seen that a higher amount of damping limits the amplitude of oscillations in the velocity and interaction force, but it takes significantly more effort for the user to move the robot. In case 3, the larger mass also takes more effort for the human to move the robot, but compared to the effects of increased damper, mass plays less of a role in the effort. Damping is the most significant cause of parasitic impedance displayed to the human, but mass still plays an important role. The higher the mass of the system the greater the amplitude of oscillation and the greater the quantity of the error between the desired drill depth and the actual depth are. Observe figure 9.

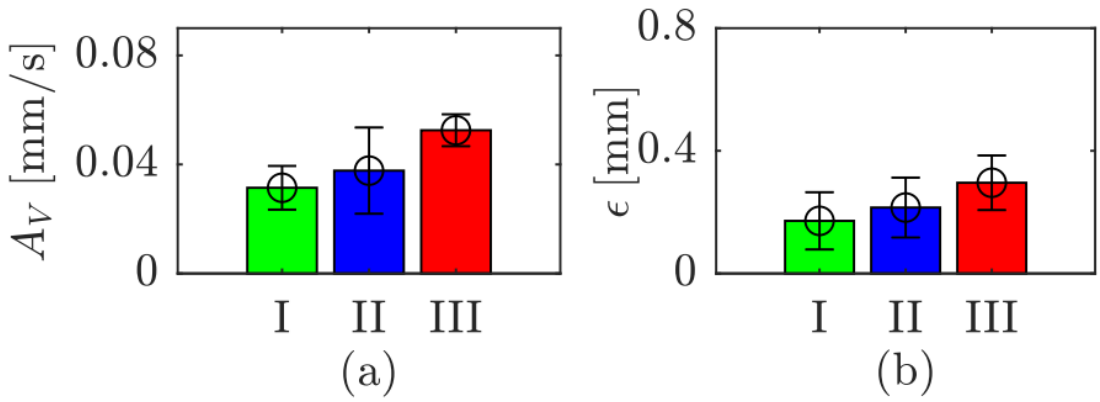

Figure 9 The magnitude of the amplitude of oscillations during the penetration phase on the left. On the right is the error between the desired drill depth and the measured drill depth.

The case with higher damping results in a more accurate drill depth and small amplitude of oscillations, as expected, but this conversely means decreased transparency. Ideally, a well-designed controller theoretically lies somewhere between Cases 1 and Cases 3 like Case 2 where the amplitude of oscillations and error are balanced with a more transparent controller with lower damping and lower mass.

7. Assessment

This paper supplies a good tool for assessing stability in hand with transparency. The combined stability and impedance cost map allow for convenient control design for any linear robotic system. The results show that values chosen in the stable region are indeed stable, and the transparency can be improved as the values of m and b are made smaller within the acceptable region in congruence with the impedance cost map. However, as the system is made more transparent, not only is stability affected, but the accuracy of the system can decrease and amplitudes in small interaction vibration also needs to be observed to ensure performance stays within acceptable bounds.

In future efforts it is pertinent that more robust stability analysis of the cobot system be undertaken. As suggested by the authors, increased damping passed certain bounds can lead to non-passive systems, where the robot may have unexpected behavior or may lead to different forms of instability. It would also be interesting to observe the controller on robots with higher DOF than 1 cartesian direction to see if the stability map concepts are well applicable, or if performance breaks down. Another interesting future work would be to see them perform more tests in a greater range of m and b in the stable region, as well as different tasks such as pick and place.

While the study provided a useful framework for controller design, some parts of the study did fall short. The analysis for stability given in the methods is lacking in detail. Given that they address stability only by observing the positivity of closed loop poles is vague and uncertain. The transfer function of the system they identified, G(s), happens to be quite high in order (15+) and in our teams' attempts to reproduce their figures with their data, the stability analysis has come back with different results than theirs. A more thorough explanation of their stability criterion would prove useful, and a more in-depth analysis of robust stability regarding disturbances, noise, etc. should be done in the future and mentioned. More tests in general with their cases 1, 2, and 3 would have allowed a more technical statistical analysis of the differences to be observed, and a comparison between the controller without admittance would have been helpful.

8. Conclusion

This paper developed a convenient framework and workflow for designing pHRI admittance controllers that can be applied to many nonlinear robotic systems. The resultant stability maps and impedance cost maps give a measurable form of evaluating transparency and verified improvement of transparency can be seen in their results. Although the stability analysis does feature less documentation than preferred and the results have yet to be reproduced. Still, our team plans to incorporate similar methods for analyzing the transparency and designing our controller for the Galen robot.

9. Readings & References

[1] Aydin, Y., Sirintuna, D., & Basdogan, C. (2020). Towards collaborative drilling with a Cobot using admittance controller. Transactions of the Institute of Measurement and Control, 43(8), 1760–1773. https://doi.org/10.1177/0142331220934643

[2] Buerger SP and Hogan N (2007) Complementary stability and loop shaping for improved human–robot interaction. IEEE Transactions

[3] Keemink AQ, van der Kooij H, Stienen AH. Admittance control for physical human–robot interaction. The International Journal of Robotics Research. 2018;37(11):1421-1444. doi:10.1177/0278364918768950

[4] Franklin, G. F., Powell, J. D., & Emami-Naeini, A. (2020). *Feedback control of Dynamic Systems*. Pearson.